INFLUENCE OF HUMIDITY AND FUEL HYDROGEN CONTENT ON ULTRAFINE NON-VOLATILE PARTICULATE MATTER FORMATION IN RQL GAS TURBINE TECHNOLOG

Andrew Crayford[1], Philip Bowen[1], Eliot Durand[1], Daniel Pugh[1], Yura Sevcenco[1], Mark Johnson[2]

1 Cardiff School of Engineering, Cardiff University, Wales, UK, CF24 3AA

2 Rolls Royce plc, Sin A-37 PO Box 31, Derby, DE24 8BJ

ABSTRACT

To address the known Local Air Quality impacts of ultrafine combustion derived soot, the International Civil Aviation Organisation (ICAO) have recently adopted a non-volatile Particulate Matter (nvPM) regulation in addition to those of NOx, UHC's and CO for civil aviation gas turbines. Increased water humidity is known to reduce the formation of NOx in flames through localised temperature reduction, however its impact on emitted nvPM is to date not clearly understood. To address this knowledge gap, nvPM formation mechanisms were assessed empirically at increasing water loadings both at atmospheric pressure - in a RQL representative optical combustor fuelled with Jet A and alternative fuel blends - and during a full-scale Rolls-Royce aero-derivative Gas Turbine test fuelled on Diesel.

In line with previous studies, in the RQL combustor rig it was observed that increased hydrogen content in the test fuel - associated with a 100% Gas-To-Liquid (GTL) derived aviation kerosene with low aromatic content (0.05%) - reduced nvPM number concentrations by an order of magnitude compared to a baseline Jet A-1 fuel with representative aromatic content (24.24%). For all fuels tested it was also observed that an elevated water loading in the primary combustion zone (≤ 0.05 kg /kg of dry air), representative of maximum global humidity levels, resulted in reductions of both nvPM number and mass concentrations of 40% and 60% respectively. During a full-scale Rolls-Royce gas turbine study similar trends were observed, with an 85% reduction in measured nvPM mass whilst water was injected into the combustor at flow rates 25% higher than the diesel fuel flow.

The nvPM reductions in both experiments are significantly larger than can be explained by water dilution effects alone, with less impact noted for fuels with higher hydrogen content. This suggests the reduction may be in part due to chemistry. Preliminary chemical kinetic investigations were undertaken using CHEMKIN-PRO and suggest that the soot reduction mechanism is potentially via a reduction in PAH formation within the flame zone. However, further analysis is required to validate if this mechanism is dominated by in-flame OH reduction mechanisms or influenced significantly by other factors associated with water dilution and reduced flame temperatures.

Keywords: Emission reduction, Particulate Matter, Alternative Fuels, Humidified Combustion.

INTRODUCTION

The World Health Organisation (WHO) estimated global premature deaths associated with air pollution to be 7 million in 2012 [1], with more recent studies indicating over 3.3 million premature deaths directly linked to fine Particulate Matter (PM2.5) [2,3]. Anthropogenic emissions of Particulate Matter from gas turbines have been shown to consist of high number concentrations of ultrafine particles (<100 nm) [4-8], analogous in morphology to those derived from the automotive sectors which have also been linked to health concerns [9,10].

To address the perceived impacts of ultrafine combustion derived soot, the International Civil Aviation Organisation (ICAO) have recently adopted a non-volatile Particulate Matter (nvPM) regulation (Annex 16; Vol: II, Appendix 7) in addition to those of NOx, UHC's and CO for civil aviation gas turbines.   In this context, nvPM is defined as any particle exiting a gas turbine engine that is found in the gas phase at a temperature of ≥350°C. In this study it is presumed nvPM consists almost entirely of solid carbonaceous particles (i.e. soot).

Currently it is estimated that aircraft only contribute 2% of global human induced CO2 emissions [11] with only a 25% contribution to airport LAQ PM2.5 [12]. However, with increasing electrification of support services and land transportation around airports, together with ever increasing demand for air transport, the contribution of aviation to LAQ issues surrounding airports is set to rise. At the same time, to address sustainable air transport, biofuel blending is considered a viable proposition, with recent preliminary studies [13,14] utilising auxiliary power unit (APU) sources demonstrating additional potential benefits for nvPM reduction and LAQ. Furthermore, the influence of ambient environmental conditions, particularly water vapour, on nvPM emissions within an RQL environment has received little attention and is poorly understood which limits the ability of regulators to propose humidity corrections for regulatory measurement analogous to those used for NOx. Nevertheless, modelled water injection in high pressure/ temperature combustion systems in the case of both diesel and GDI automotive reciprocating engines has been shown to reduce soot & NOx emissions via thermal, dilution & chemical effects [15,16].

The aim of this study is to investigate experimentally potential routes to nvPM reduction in gas turbine environments through the influence of hydrogen content either within the fuel, or in the form of water in the primary flame zone of a representative RQL gas turbine diffusion flame. First, changes in nvPM formation characteristics were investigated for various blends of Jet A-1 & GTL fuel and a Jet A-1 & Camelina derived Hydro-processed Esters and Fatty Acids (HEFA) fuel at varying equivalence ratios. Secondly, variation of hydrogen content via changes in the primary-air humidity were studied experimentally and numerically to analyse the influence of water-fraction on soot formation. An OH* chemiluminescence relative intensity measurement at each flame condition was taken in a generic optical combustor to act as a qualitative measure of inflame OH concentration. Finally, the results were numerically analysed by correlating nvPM characteristics against established predictors of nvPM generation and destruction.

1 Experimental Facilities

Experiments were conducted in a centrally fired diffusion swirl burner housed within a High-Pressure Optical Combustor (HPOC) modified from previous studies [17, 18]. The burner and casing assembly are shown in Fig. 1. A fuel delivery lance (Fig. 1-a) delivered liquid fuel to a Danfoss 45° hollow cone (2.0 US gal/hr) pressure-swirl nozzle. Preheated air provided from an Atlas Copco GA-45VSD compressor, dried to a dew point of -17°C using a Beko Drypoint DPRA960, enter an inlet plenum (Fig. 1-b) in the case of humidity tests, steam was also mixed at this position. Air flowrates were quantified using Coriolis mass-flow meters (Emerson CMF025M ±0.35%). During the humidity experiments, steam was supplied using a heated line (Winkler WAMX1537), with the burner conditioned to operational temperature using preheated air prior to combustion. Water supply was regulated using a secondary mass flow controller (Bronkhorst mini CORI-FLOW (±0.2%)) and pre-vaporised in electrical heaters (Watlow CASTX-4.5kW). After entering the plenum, reactants travel through the premix chamber (Fig. 1-c) to a single radial-tangential swirler (Fig. 1-d) and out the burner exit nozzle (20 mm radius). The outlet has a geometric swirl number equivalent to $Sg = 0.8$. Optical access is afforded, via four diametrically opposed, quartz windows housed within the HPOC with flame chemiluminescence signal captured from above. The burner was operated within a cylindrical quartz tube, at a fixed expansion ratio of 2.5 from the burner nozzle exit (Fig. 1-e). Secondary air for staged combustion was introduced through the casing inlet, flowing around the quartz tube.
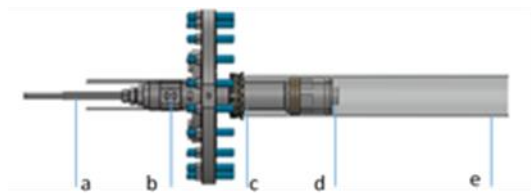

FIGURE 1: BURNER SCHEMATIC

1.1 nvPM Emissions Measurements

The nvPM emissions measurement system used in this study was the European mobile nvPM reference system designed at Cardiff University and operated on behalf of the European Union Aviation Safety Agency (EASA) [4] in accordance with relevant standards (ICAO Annex 16 Vol: II Appendix 7, and SAE ARP6320). Exhaust products were sampled downstream of the secondary air stage via a 9-point equal area probe connected to a water-conditioned heat exchanger used to regulate the sample temperature to 433 K. The thermally conditioned sample was subsequently transferred via a 2 m (8 mm ID) antistatic PTFE heated line also maintained at 433 K, to a Dekati DI-1000 ejector diluter which nominally diluted the exhaust sample by a factor of 10 whilst cooling it to 333 K. The exhaust was then transferred at a nominal flow rate of 25 sLPM, via a 25 m (8 mm ID) antistatic PTFE heated line (333 K) to a 1000 nm sharp cut-point cyclone prior to the measurement analysers.

Concentrations of nvPM number were measured using a suitably calibrated AVL Aviation Particle Counter (APC), which employs dilution and catalytic volatile removal before measurement with a butanol-based Condensation Particle Counter (CPC) with a >50% counting efficiency at 10 nm and >90% counting efficiency at 15 nm. The nvPM mass was measured using both an AVL Micro Soot Sensor (MSS) and Artium LII-300 analyser, which are extractive instruments which employ photoacoustic and laser-induced incandescence principles respectively. The measured volumetric

nvPM concentrations were then converted to an Emission Index (EI) as per the recommendations of SAE AIR6241, representing the measured pollutant emission per kg of fuel combusted. This was facilitated by the measurement of CO2 pre and post dilution using a two channel Rosemount NDIR analyser operated in accordance with SAE ARP 1256. Other exhaust gases were also measured but are not discussed further at this time.

In addition to nvPM mass and number quantification, particle size distributions were measured using a real time, Cambustion Differential Mobility Sizer (DMS-500), which was calibrated against a surrogate agglomerate soot source

1.1   OH* Chemiluminescence

2D chemiluminescent measurements of the excited hydroxyl intermediate radical (OH*) were undertaken on the primary diffusion flame using an established technique [19]. For each experiment, two hundred intensified, centred images (~100 x ~75 mm in radial and axial planes) were recorded at a rate of 10 Hz with intensities calculated by applying an averaging algorithm and background correction, in accordance with principles proposed in previous studies [17, 19]. These images were subsequently analysed to determine the peak OH* signature to assess flame location and inflame OH concentrations.

2 Experimental conditions

To simplify the test schedule and remove the uncertainty of particle losses associated with the operation of a water-cooled variable area back pressure valve, all combustion tests were performed at atmospheric pressure. Similarly, the air inlet temperature was kept nominally constant at 540 K, with a standard deviation of 7 K across all tests. Secondary air flows used to simulate the quench stage of a RQL combustion system were also kept constant at 80 g/s (±0.2 g/s) for all conditions tested. Air Fuel Ratio (AFR) quoted in this study are representative of the primary diffusion flame zone which corresponded to nominal powers of circa 100 kW.

Four Jet A-1 / GTL blends supplied by Shell Petrochemicals were investigated in this study at nominal concentrations of 100% Jet A-1, 50% GTL, 75% GTL and 100% GTL with their fuel properties presented in Table 1. In addition, an Initiative Towards sustAinable Kerosene for Aviation (ITAKA), JET A-1 and Camelina derived HEFA fuel blend, with specifications detailed in Table 1, was tested providing a comparison to the 50% GTL case which had a similar chemical composition although formulated using a different feedstock and synthesis technique.

3 Results

3.1 Fuel Effects

The effect of hydrogen content within the fuel was tested across a range of primary diffusion flame AFR's. As seen in Fig. 2, pure Jet A-1 fuel generated the highest number concentrations of nvPM across all power conditions, with increasing concentrations of GTL or HEFA (ITAKA) fuel reducing the measured concentrations. Fig. 3 presents the fuel effect data as a function of Hydrogen content fitted with exponential correlations to aid visualisation of the trends ($0.70 \leq R^2 \leq 0.95$). A decrease in EI number is observed with increasing hydrogen content for all AFRs (Table 1) is symptomatic of reducing aromatic concentrations in alternative fuels. An order of magnitude reduction in EI number is experienced with the highest hydrogen content pure GTL fuel (H_2 % = 15.47) compared to the base

Jet A-1 fuel which had the lowest hydrogen content (H_2 % = 13.427). Progressively lower nvPM emissions are noted for fuels of increasingly higher hydrogen content or volumes of alternative fuel, independent of fuel processing method. It is noted that similar nvPM EI mass reductions were also observed with increasing hydrogen content and AFR. Graphical depictions are not presented at this time due to large scatter in the mass data, thought to be attributed to random shedding of large particles from the combustor wall during the perceived stable operating condition (average coefficient of variation over the 30-seconds stable condition of 12.8% for nvPM mass & 3.0% for nvPM number).

The results presented in this study agree with previous studies investigating the effect of alternative fuels on nvPM emissions from gas turbines [6, 13, 14, 20, 21] which also reported reductions in nvPM number, mass number and particle size with increasing levels of alternative fuel (hydrogen content).
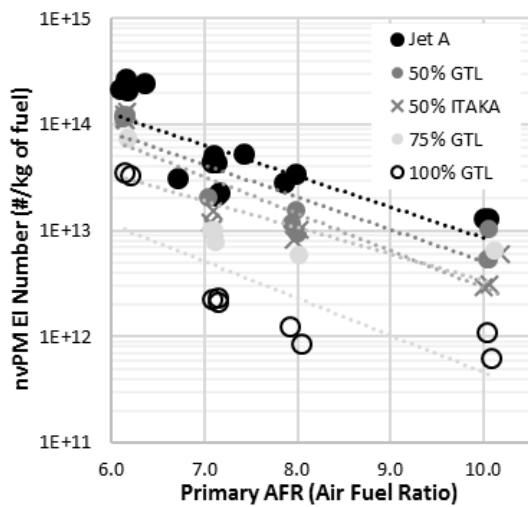

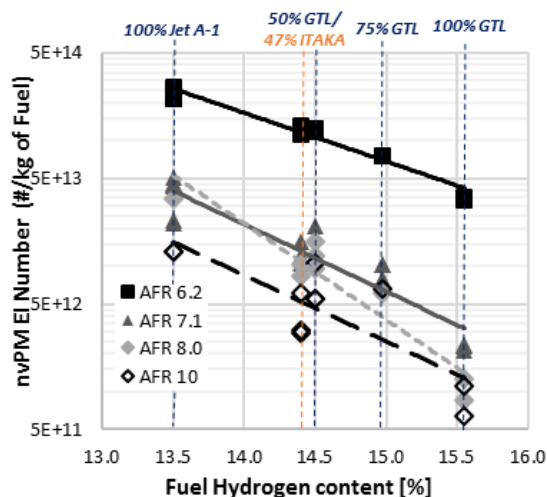FIGURE 2: nvPM EI NUMBER CONCENTRATIONS AT DIFFERENT PRIMARY AFR'S FOR JET-A AND GTL BLENDS

FIGURE 3: nvPM EI NUMBER CONCENTRATIONS AT DIFFERENT FUEL HYDROGEN CONTENTS FOR DIFFERENT AIR TO FUEL RATIOS

TABLE 1: FUEL COMPOSITION OF THE JET-A AND ALTERNATIVE FUELS TESTED

| Fuel	Result Heading	Method	Units	Jet A-1	50% GTL	75% GTL	100% GTL	47% HEFA
					GTL Shell blends			ITAKA blend
COMBUSTION	Naphthalene	ASTM D 1840	(%V/V)	0.81	0.63	0.25	<0.08	0.59
	Smoke point	ASTM D 1322	(mm)	19.0	28.0	>50.0		35.5
	Specific energy	ASTM D 3338	(MJ/Kg)	43.013	43.577	43.864	44.25	43.340
COMPOSITION	Aromatics (%mass)	IP 436/ ASTM D 6379	%m	20.8		5.3		
	FIA Aromatics	ASTM D 1319/IP 156	(%V/V)		10.9			9.2
	Mercaptan sulphur	ASTM D 3227/IP 342	(%m/m)	0.0003	<0.0003	<0.0003	<0.0003	
	Total sulphur	ASTM D 2622	(%m/m)	0.0036		0.0025		0.070
	Total sulphur	IP 336	(%m/m)	<0.01		<0.01		
	Sulphur content	ASTM D 5453	mg/kg				<1.0	
	Sulphur content	ASTM D 4294	%m					
	Total aromatics	Inhouse	(%wt)	24.24	12.11	6.71	0.05	
	H content (calc)	ASTM D 5291 GC x GC	(%wt)	13.427	14.426	14.895	15.47	14.403
	H/C ratio (calc)	ASTM D 5291 GC x GC	mole/mole	1.861	2.023	2.100	2.196	2.006
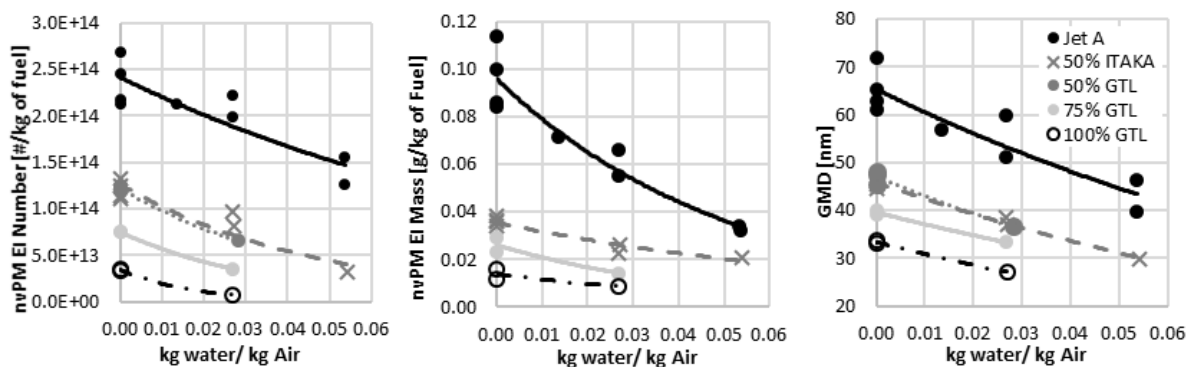
FIGURE 4: nvPM EI NUMBER, MASS, AND GEOMETRIC MEAN DIAMETER (GMD) FITTED WITH EXPONENTIAL CORRELATIONS AT INCREASING WATER LOADINGS FOR DIFFERENT FUEL BLENDS (AFR 6.2)

3.2 Water Effects (Experimental and Numerical)

The effect of water on nvPM production in the diffusion flame was investigated by introducing sequentially more steam into the primary combustion zone compared to the dry base case, before returning to a repeated dry case to ensure rig conditions had not affected nvPM production. As can be seen in Fig. 4 for all the fuel blends investigated, increased water loadings resulted in reductions of nvPM number, mass and particle size with exponential fits added to aid visual interpretation of the trends ($0.78 \leq R^2 \leq 0.99$).

There is 20% scatter in repeated Jet A-1 experiments for the dry case, which occurred over a 5-day testing period. This uncertainty is comparable to scatter experienced in other test programmes [4] probably resulting from subtle variations in rig operation conditions (e.g. temperature, pressure, AFR etc.) and measurement drift. For the Jet A-1 data presented in Fig. 4, 40 and 65% reductions in EI number and mass respectively are observed over the water loading range considered. Similarly, a

corresponding reduction in measured GMD from 65 to 45 nm was observed, suggesting the water was either suppressing soot formation in the flame front or reducing soot concentrations in the post flame boundary. These reductions are significantly greater than the expected reductions associated with dilution given the relatively low levels of water compared to total reactants (0.008 kg/kg).

Distributions of particle size are not presented at this time but generally exhibited a dominant 'lognormal' agglomeration peak (>30 nm) corresponding to the main nvPM mode, with a small nucleation shoulder (10-20 nm) also observed which is thought to originate from unburnt fuel found in the exhaust due to inefficiencies in the combustor rig used.
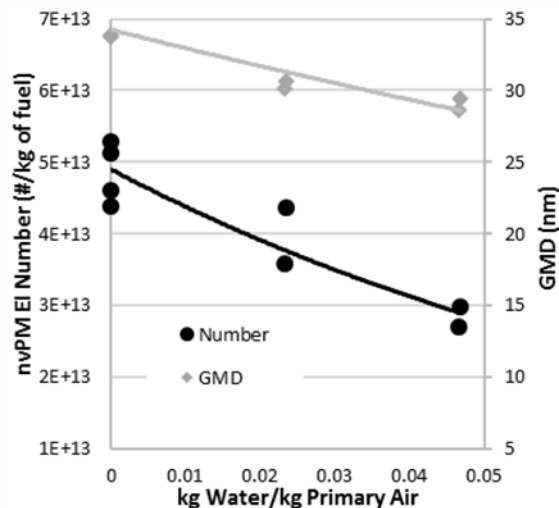
FIGURE 5: nvPM EI NUMBER AND GMD AT INCREASING WATER LOADINGS (AFR 7.1)

As can be seen in Fig. 5, for a leaner Jet A-1 flame with a local AFR of 7.1, a similar 40% reduction in EI number was observed, with an associated 18% reduction in measured GMD.

It is noted that nvPM number and mass emissions reported in this work are not corrected for size-dependent loss occurring in the compliant sampling & measurement systems as discussed in SAE ARP 6481. Hence, when a reduction in GMD is associated with the reported reductions in nvPM emissions, the corresponding reduction at the engine exit plane may appear amplified. However, this would not change the general trends reported in this study.

3.3 Chemical Kinetics Modelling

Chemical kinetics were modelled using the Diffusion Flamelet Generator in CHEMKIN-PRO to interrogate changes in intermediate chemistry alongside the changes in nvPM observed with increased primary air humidification. The model was specified for a nominal range of stoichiometric scalar dissipation rates (SDDR) equivalent to 1-0.0001 s-1 with an adaptive grid. Dumped energy was used for the initial profile estimate and a minimum flame temperature of 1500 K. Fuel was supplied separately to air / H_2O to simulate changes in equivalent experimental conditions. A surrogate mixture was employed, as specified by Saffaripour et al. [23] and others [24] for the investigation of soot formation with Jet A-1 flames, comprising molar fractions of 69% n-decane ($C_{10}H_{22}$) 20% n-propylbenzene and 11% (C_9H_{12}) n-propylcyclohexane (C_9H_{18}). Each simulation employed the Jet-A1 reaction mechanism developed by Saffaripour et al. [23] consisting of 248 chemical species and 2089 reactions. Three distinct simulations were performed, one with dry air (WL0), an intermediate

humidified fraction (WL1 – equivalent to a 3.59%mol in air) and the equivalent wettest experimental condition (WL2 – equivalent to a 6.97%mol in air). All results are presented for equivalent nominal SDDR=1 s-1, with an inlet temperature of 540 K.

A comparison between flame temperature and OH fraction is presented with each humidified loading in Fig. 6. Where a mixture fraction of 0 corresponds to 100% air, transitioning through the 1-D diffusion flamelet to 100% fuel. As would be expected, lower peak flame temperatures are modelled at higher water concentrations, providing a drop of ~90 K for specified experimental conditions. Bhatt and Lindstedt [25] demonstrated how OH facilitates soot reduction in flames, as given by:

$C_{s,i} + OH \rightarrow C_{s,i-1} + CO + H,$
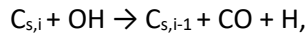
Where, $C_{s,i}$ denotes a soot particle containing i carbon atoms.

However, the simulations employed predicted a reduction in peak OH fraction with increasing humidified loading, signifying a relative reduction in concentration. A comparison was also made between maximum measured OH* chemiluminescence intensities - examples for half flames are presented in Fig. 7(a) (x=0 mm on the burner centreline) with the captured 200 raw-image average and equivalent Abel-transformed planar image Fig. 7(b) [17]; the colourmap is normalised to the equivalent intensity distribution for the dataset maximum (from the dry image).

The reduction in OH* chemiluminescence resulting from water addition is evident from the fall in measured intensities, and is more significant than the simulated changes in OH fraction from Fig. 6 (equivalent to ~58%). The greater reduction in chemiluminescence intensity results from a fall in temperature, quenching the emission of light from the excited radical, and cannot be attributed to a reduction in OH fraction alone (similar effects have been recently observed with steam used for atomization and compared with air [26]). Nevertheless, these preliminary trends suggest OH is not likely to be dominating nvPM reductions from the addition of H_2O.
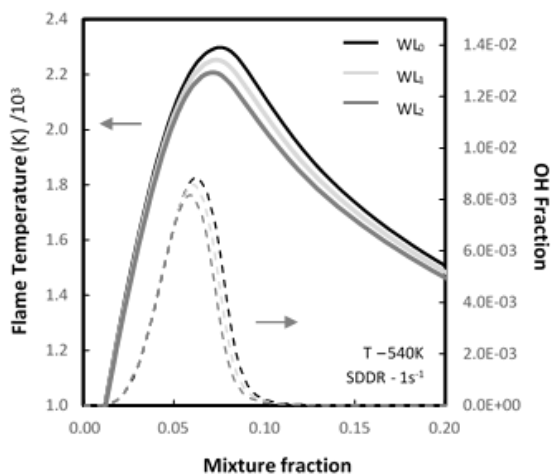

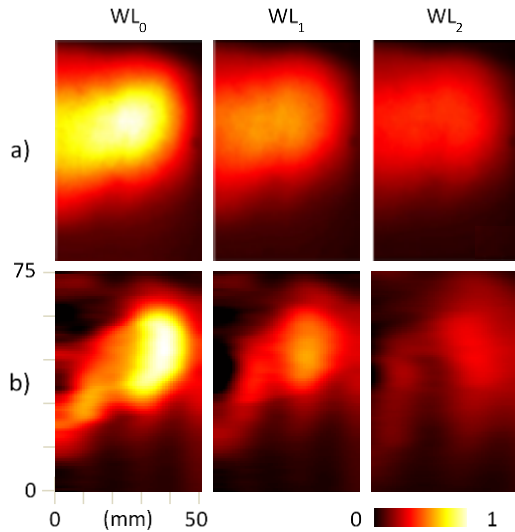FIGURE 6: MODELLED CHANGES IN FLAME TEMPERATURE (SOLID) AND OH FRACTION (DOTTED) FOR INCREASING WATER LOADINGS.

FIGURE 7: MEASURED OH* CHEMILUMINESCENCE FOR (a) THE RAW AVERAGED 200-IMAGE DATASET (b) EQUIVALENT ABEL TRANSFORM

The models also predicted changes in sample PAH fractions, namely; benzene (C_6H_6), pyrene ($C_{16}H_{10}$) and naphthalene ($C_{10}H_8$) as well-established soot precursors [23]. The change in concentration with reactant mixture fraction (air = 0, and Jet A-1 surrogate = 1) is plotted for the 1D flamelet in Fig. 8.

Peak reductions in all three species are evident for increasing water fraction, with a ~6.1% reduction for pyrene, and ~3% for the other two. The models therefore suggest that in addition to reducing temperature, increased humidity is potentially suppressing PAH fractions. This subsequently reduces nvPM formation via the PAH formation mechanism, possibly more influential than the influence of OH, and leading to the reduction in measured concentrations. However, it is emphasised that only preliminary trends have been identified and this requires further detailed study.
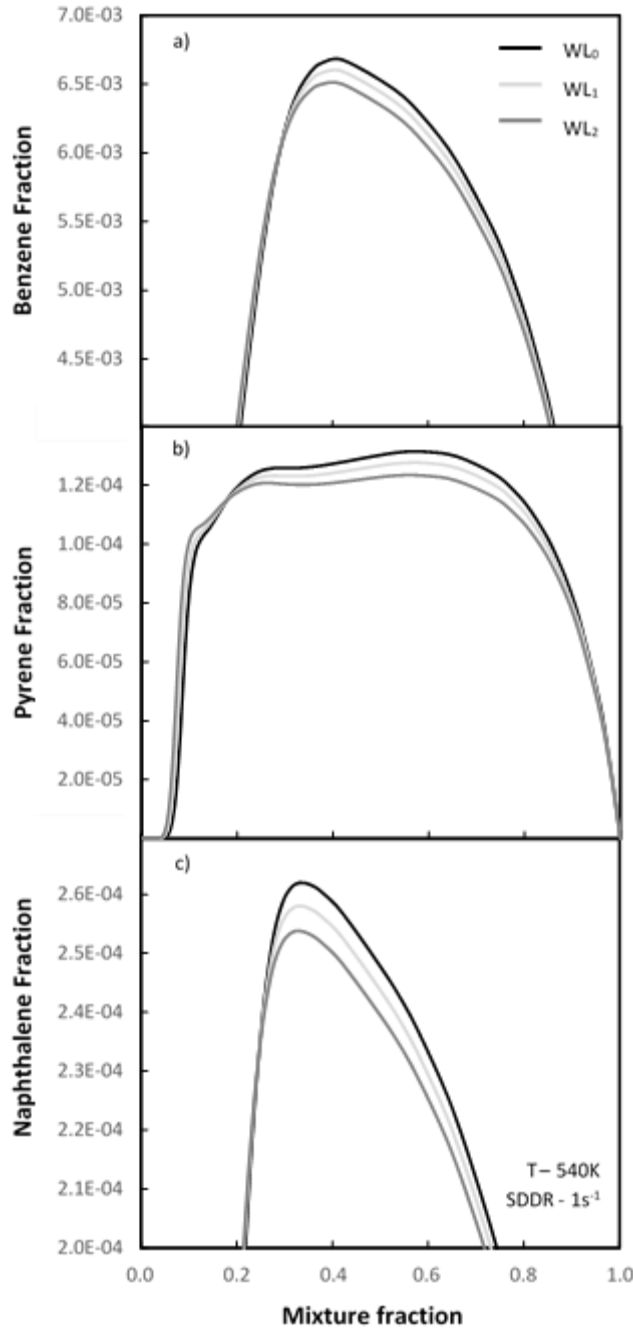
FIGURE 8: PREDICTED CHANGES IN BENZENE (a), PYRENE (b) AND NAPHTHALENE (c)
CONCENTRATION PROFILES IN THE JET A-1 DIFFUSION FLAMELET

3.4 Full Scale Water Injection Validation

For decades the impact of water addition in aero-derivative gas turbines has been successfully
demonstrated with a view to increasing power output [27,28] and reduced NOx, however, to date
the impact on nvPM emissions has not been reported. It is noted that water addition has been
achieved in different ways; namely injection into the compressor section [27] as was simulated in
the combustor rig experiment discussed earlier (Section 3.2) or via direct injection into the
combustion chamber [28]. To investigate the effect of increased water loadings on nvPM emissions
at full-scale, a water injection test was conducted on a land-based power generation Rolls-Royce

Trent architecture gas turbine engine, fuelled on diesel. In this case water was directly injected into the combustion chamber as detailed in other studies [28]. The impact of water addition on nvPM mass was quantified using an extractive Artium LII-300 instrument. For proprietary reasons, fuel and water flowrates are normalised to maximum water flow rate and plotted against normalised combustor inlet pressure (P30) and temperature (T30) in Fig. 9, which presents a period of stable engine power with increasing water loading.

As can be seen during this stable engine power condition, water flow was increased up to a flow rate 25% higher than the corresponding fuel flow. This increase in water resulted in an 85% reduction in measured mass concentration being observed, in agreement with the trends of the laboratory findings (Section 3.2) and demonstrating the reductive properties of water on soot formation in the primary combustion zone in a real-world application.
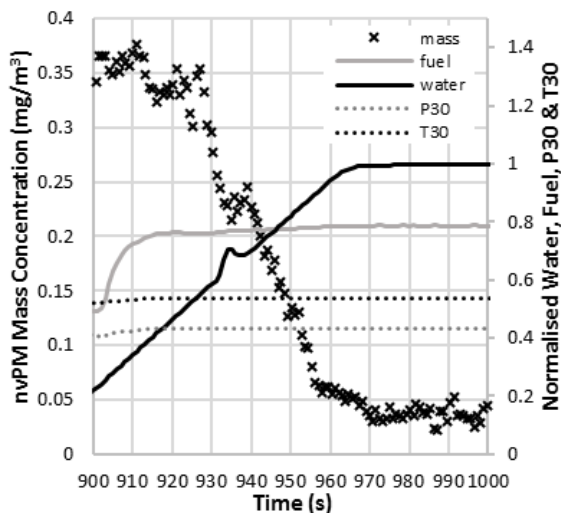

FIGURE 9: nvPM MASS CONCENTRATION MEASURED AT CONSTANT ENGINE POWER AT VARYING WATER LOADING

3.5 Full Scale Air Humidity Validation

Full-scale gas turbine engine data relating humidity to nvPM is believed not to be previously reported, hence it is difficult to interpret whether the reductions in measured nvPM observed in this study are also witnessed in high pressure RQL combustors experiencing humidity fluctuations in both the rich and quench zones. Emission measurements repeated over multiple test days as part of the SAMPLE programme [4] on two engines variants namely Single Annular Combustor (SAC) and Dual Annular Combustor (DAC) provide limited data linking nvPM to relative ambient humidity.   The results presented in Fig. 10 & 11, display EI Number measured by a Cambustion DMS-500 against measured humidity presented as kg of water / kg of dry air entering the engine.

It is noted that for the range of humidity experienced during the weeklong test, there was no observable trend linking ambient air humidity to nvPM number concentration for either engine type. This observation may in part be associated with reductions in primary soot formation being offset by reduced soot burnout likely experienced in the cooler quench zone of higher humidity cases. However, it is also noted that the deviation in humidity realised on the full engine were significantly smaller (by a factor of 10) than those tested as part of this test programme, and hence only limited

reductions in EI nvPM would be expected, which would likely be within the uncertainty of repeated day-to-day test points. As observed in Fig. 4(a), nvPM number variations on the repeated dry cases are typically larger than the predicted reductions in nvPM expressed by the exponential fit, hence further validation on large-scale engines with higher variations in ambient humidity are required.
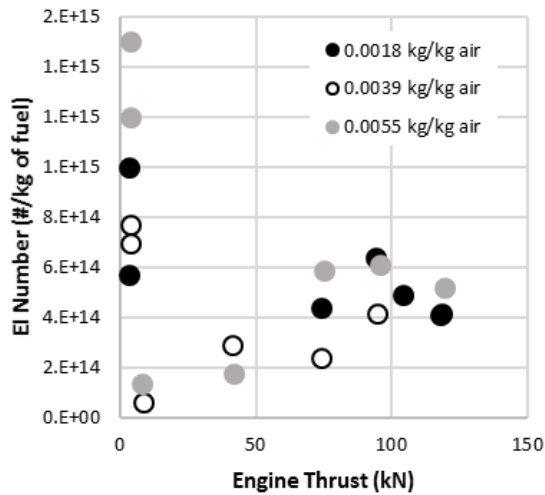

FIGURE 10: nvPM EI DATA SAC ENGINE AT VARYING LEVELS OF ATMOSPHERIC HUMIMDITY [4]
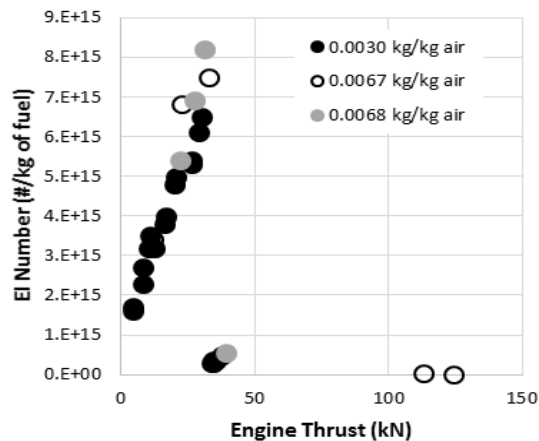

FIGURE 11: nvPM EI DATA DAC ENGINE AT VARYING LEVELS OF ATMOSPHERIC HUMIMDITY [4]

CONCLUSION

Experimental investigations of fuel and humidity effects on nvPM reduction have demonstrated that increased hydrogen within the diffusion combustion zone from either the fuel or humidity results in a reduction in measured nvPM number, mass and size. Increased volumes of hydrogen content (low aromatic content) fuels have been shown to reduce measured EI number concentrations by an order of magnitude, which demonstrates the potential to improve LAQ surrounding airports now and in the future.

Laboratory and full-scale engine tests have correlated nvPM reductions with increased volumes of water in the primary rich zone, independent of how the water is added (in combustion air or direct injection into combustion chamber). However, for the limited cases of full-scale aero-engine emissions testing, small variations in water loading witnessed day-to-day as relative humidity variation in both the rich and quench zones, did not display any observable reductions in nvPM greater than the scatter typically associated with nvPM repeat measurements.

Chemical kinetic simulations suggest the mechanism for soot reduction associated with increased humidity is via a reduction in PAH in the flame zone, however further work is required to understand whether this mechanism is influenced by in flame consumption via OH and O radicals and/or local reductions in flame temperature.

REFERENCES

[1] World Health Organisation Press Release, Geneva, https://www.who.int/mediacentre/news/releases/2014/air-pollution/en/ (25th March 2014)

[2] Lelieveld, J., Evans, J., Fnais, M. et al. "The contribution of outdoor air pollution sources to premature mortality on a global scale", Nature 525, 367–371 (2015)

https://doi.org/10.1038/nature15371

[3] Zhang, Q., Jiang, X., Tong, D. et al. "Transboundary health impacts of transported global air pollution and international trade". Nature 543, 705–709 (2017).

https://doi.org/10.1038/nature21712

[4] Crayford et al. "Studying, sAmpling and Measuring of aircraft ParticuLate Emissions III", EASA (2013)

[5] Olfert et al. "Effective density and volatility of particles sampled from a helicopter gas turbine engine", Aerosol Science and Technology (2017), 51:6, 704-714,

https://doi.org/10.1080/02786826.2017.1292346

[6] Lobo et al. "Demonstration of a Regulatory Method for Aircraft Engine Nonvolatile PM Emissions Measurements with Conventional and Isoparaffinic Kerosene fuels" Energy Fuels (2016), 30, 7770–7777

https://doi.org/10.1021/acs.energyfuels.6b01581

[7] Yu et al. "Evaluation of PM emissions from two in-service gas turbine general aviation aircraft engines" Atmospheric Environment 160 (2017)

https://doi.org/10.1016/j.atmosenv.2017.04.007

[8] Abegglen et al. "Effective density and mass–mobility exponents of particulate matter in aircraft turbine exhaust: Dependence on engine thrust and particle size" Journal of Aerosol Science (2015) 135–147

https://doi.org/10.1016/j.jaerosci.2015.06.003

[9] Knibbs et al. "A review of commuter exposure to ultrafine particles and its health effects" Atmospheric Environment Volume 45, Issue 16, (2011), Pages 2611-2622

https://doi.org/10.1016/j.atmosenv.2011.02.065

[10] Losacco, C. & Perillo, A. "Particulate matter air pollution and respiratory impact on humans and animals", A. Environ Sci Pollut Res (2018) 25: 33901 https://doi.org/10.1007/s11356-018-3344-9

[11]Air Transport Action Group, ATAG "Facts & figures" http://www.atag.org/facts-and-figures.html (2017)

[12] Heathrow Airport - Air Quality Assessment (2013)

[13] Lobo et al. "Evaluation of Non-volatile Particulate Matter Emission Characteristics of an Aircraft Auxiliary Power Unit with Varying Alternative Jet Fuel Blend Ratios" Energy Fuels (2015), 29, 7705–7711

https://doi.org/10.1021/acs.energyfuels.5b01758

[14] Schripp et al. "Particle emissions of two unblended alternative jet fuels in a full scale jet engine", Fuel (2019), Vol. 256 https://doi.org/10.1016/j.fuel.2019.115903

[15] Ma et al. "Effects of Intake Manifold Water Injection on Combustion and Emissions of Diesel Engine", Energy Procedia (2014), Vol. 61, Pages 777-781

https://doi.org/10.1016/j.egypro.2014.11.963

[16] Mingrui et al. "Water injection for higher engine performance and lower emissions", Journal of the Energy Institute (2017), Vol. 90, Issue 2, Pages 285-299

https://doi.org/10.1016/j.joei.2015.12.003

[17] D. Pugh et al. "Dissociative influence of H_2O vapour/spray on lean blowoff and NOx reduction for heavily carbonaceous syngas swirling flames" Combust. Flame 177 (2017) 37-48

https://doi.org/10.1016/j.combustflame.2016.11.010

[18] D. Pugh et al. "Catalytic Influence of Water Vapor on Lean Blow-Off and NOx Reduction for Pressurized Swirling Syngas Flames" J. Eng. Gas Turbines Power (2017)

https://doi.org/10.1115/1.4038417

[19] J. Runyon et al. "Lean methane flame stability in a premixed generic swirl burner: Isothermal flow and atmospheric combustion characterization" Exp. Therm. Fluid Sci. (2017)

https://doi.org/10.1016/j.expthermflusci.2017.11.019

[20] Christie et al. "Gas Turbine Engine Nonvolatile Particulate Matter Mass Emissions: Correlation with Smoke Number for Conventional and Alternative Fuel Blends" Environ. Sci. Technol. (2017), 51 (2), pp 988–996

https://doi.org/10.1021/acs.est.6b03766

[21] Moore et al. "Influence of Jet Fuel Composition on Aircraft Engine Emissions: A Synthesis of Aerosol Emissions Data from the NASA APEX, AAFEX, and ACCESS Missions" Energy Fuels, 29 (4), pp 2591–2600 (2015)

https://doi.org/10.1021/ef502618w

[22] Moore et al. "Biofuel blending reduces particle emissions from aircraft engines at cruise conditions" Nature 543, 411–415 (2017) https://doi.org/10.1038/nature21420

[23] Saffaripour et al. "Experimental investigation and detailed modeling of soot aggregate formation and size distribution in laminar coflow diffusion flames of Jet A-1, a synthetic kerosene, and n-decane" Combustion and Flame, Volume 161, Issue 3, (2014), 848-863

https://doi.org/10.1016/j.combustflame.2013.10.016

[24] Dagaut et al. "Chemical Kinetic Study of the Effect of a Biofuel Additive on Jet-A1 Combustion" J. Phys. Chem. A (2007), 111, 19, 3992-4000 https://doi.org/10.1021/jp067525j

[25] J.S. Bhatt & R.P. Lindstedt, "Analysis of the impact of agglomeration and surface chemistry models on soot formation and oxidation" Proceedings of the Combustion Institute 32 (2009) 713–720 https://doi.org/10.1016/j.proci.2008.06.201

[26] Jozsa, V. & Sztanko, K. "Flame emission spectroscopy measurement of a steam blast and air blast burner", Thermal Science 21, (2), (2017) 1021-1030

https://doi.org/10.2298/TSCI150616062J

[27] PPS Group "SIEMENS INDUSTRIAL TRENT 60" http://www.maya.design/pss/product/siemens-industrial-trent-60/ accessed 29th Jan 2020

[28] Modern Power Systems Press release (23 May 2004), https://www.modernpowersystems.com/features/featurewater-injection-takes-trent-to-58-mw/ accessed 29th Jan 2020